Two-photon microscopy on vital corotid arteries: imaging the relation between collagen and inflammatory cells in atherosclerotic plaques

Two-photon microscopy on vital carotid arteries: imaging the relationship between collagen and inflammatory cells in atherosclerotic plaques

Remco T. A. Megens
Maastricht University
Cardiovascular Research Institute Maastricht
Department of Biomedical Engineering
Universiteitssingel 50
6229 ER, Maastricht, The Netherlands

Mirjam G. A. oude Egbrink
Maastricht University
Cardiovascular Research Institute Maastricht
Department of Physiology
Universiteitssingel 50
6229 ER, Maastricht, The Netherlands

Maarten Merkx
Dick W. Slaaf
Technical University Eindhoven
Department of Biomedical Engineering
P.O. Box 513
5600 MB, Eindhoven, The Netherlands

Marc A. M. J. van Zandvoort
Maastricht University
Cardiovascular Research Institute Maastricht
Department of Biomedical Engineering
Universiteitssingel 50
6229 ER, Maastricht, The Netherlands

Abstract. We used two-photon laser scanning microscopy (TPLSM) to demonstrate for the first time its potential in studying relational details at the cellular level of atherogenesis in intact, viable mouse carotid arteries. Isolated and mounted arteries of ApoE-/-mice, aged 15 or 21 weeks (7 and 13 weeks on western diet), were imaged after labeling with specific fluorescent markers for cell nuclei, inflammatory cells, collagen, and lipids. Data were compared with C57BL6/J mice fed a chow diet. Control vessels had intact endothelium without adhering blood cells or significant intimal collagen labeling. In ApoE-/-mice already at 15 weeks, inflammatory cells adhered to the endothelium and increased labeling of collagen was observed in tunica intima at both lesion-prone and non-lesion-prone sites, indicating endothelium activation. In plaques, internalized inflammatory cell density increased with age and plaque progression in tunicae adventitia and intima, but not media. In the whole plaque, aging or plaque progression did not alter the direct relationship between inflammatory cells and collagen. However, within the fibrous caps specifically, direct contact between inflammatory cells and collagen increased with age. This study demonstrates the potential of TPLSM in determining detailed information regarding the complex relationship between inflammatory cells and collagen during atherogenesis. [DOI: 10.1117/1.2965542]

Keywords: two-photon microscopy; atherogenesis; collagen; inflammatory cells.

Paper 07399R received Oct. 8, 2007; revised manuscript received Feb. 10, 2008; accepted for publication Mar. 6, 2008; published online Aug. 25, 2008.

1 Introduction

Vulnerable plaques are the major cause of acute clinical complications of atherosclerosis.[1] Vulnerable plaques can rupture and cause a thrombotic reaction that can occlude the (downstream) artery, which may result in stroke or myocardial infarction.[2] Major determinants of vulnerability of human atherosclerotic plaques are extracellular matrix content and extent of inflammation.[1,3,4] Stable plaques have a large collagen content and are mostly surrounded by a thick, collagen-rich fibrous cap.[5] Loss of collagen reduces the tensile strength of the fibrous cap and increases the probability of rupture.[6,7] Atherosclerotic plaques also contain inflammatory cells such as macrophages that are known to produce enzymes like matrix metalloproteinases that break down extracellular matrix proteins such as collagen and inhibit collagen synthesis by smooth muscle cells.[4,8,9] It is generally accepted that as a result, the stability of atherosclerotic plaques may be affected.[2,10] Indeed, histological studies revealed that collagen-poor and inflammation-rich plaques are more likely to rupture.[10]

Mouse models of atherosclerosis, such as apolipoprotein E knockout mice ($ApoE^{-/-}$), are advantageous for studying the (chronic) process of atherogenesis. However, most of the present knowledge on atherosclerosis in such models is still obtained by histological studies using sliced, fixated nonviable arteries. Only little is known of the 3-dimensional organization of the arterial wall in intact and viable large arteries containing atherosclerotic plaques. Such data will provide new insight into plaque structure and the relationship and mutual influence between inflammatory cells and collagen in plaques throughout their development.

Two-photon laser-scanning microscopy (TPLSM) combines large penetration depth with subcellular resolution, also in deeper layers.[11] Its good optical sectioning properties, good sensitivity, and high (fluorescent) contrast enabled 3-dimensional imaging at the subcellular level of large mouse arteries mounted and pressurized in a perfusion chamber, maintaining their physiological structure, viability, and functionality for several hours[12,13] or in a non-mounted setting.[14–17]

In this study, TPLSM was applied on mounted arteries labeled with specific, vital fluorescent markers for collagen,[13,18] inflammatory cells, cell nuclei, and lipids to gain

Address all correspondence to Marc A. M. J. van Zandvoort, Tel:+31-43-3881665; Fax:+31-43-3670916; E-mail: MAMJ.vanzandvoort@bf.unimaas.nl

1083-3668/2008/13(4)/044022/10/$25.00 © 2008 SPIE

insight into the distribution of collagen and its association with inflammatory cells during atherogenesis.

2 Materials and Methods

2.1 *Animals*

Experiments and procedures were approved by the local ethics committee on the use of laboratory animals. Experimental groups consisted of C57BL6/J control mice [14–16 weeks (n=7), 20–22 weeks (n=7)] and atherosclerosis-prone ApoE$^{-/-}$ mice [14–16 weeks (n=7), 20–22 weeks (n=6)]. Mice were obtained from Charles River, Maastricht, the Netherlands. ApoE$^{-/-}$ mice were fed a western diet starting at the age of 8 weeks (WD4021.06; Hope Farms, Woerden, the Netherlands), while C57BL6/J controls were fed a chow diet (SSNIFF; Bioservices, Uden, the Netherlands). Mice were euthanized by a mixture of CO_2 and O_2, after which carotid artery segments (common part and bifurcation) were excised.

2.2 *Tissue Preparation and Staining*

Excised carotid arteries, including bifurcation, were mounted in a perfusion chamber.[12,13] Side branches were ligated. The system was filled with Hanks Balanced Salt Solution (HBSS, pH 7.4) containing in mmol/l: NaCl 144, HEPES 14.9, glucose 5.5, KCl 4.7, $CaCl_2$ 2.5, KH_2PO_4 1.2, and $MgSO_4$ 1.2. On average, intraluminal pressure was 50 mmHg (depending on the maximum pressure ligations could endure). All fluorescent markers were dissolved in HBSS and administered both intra- and extraluminally. Incubation started 30 minutes prior to the start of image acquisition. Probes remained present during image acquisition, since this did not alter their labeling characteristics or the viability of arteries, nor reduce the image quality.

DNA/RNA markers SYTO41 ($\lambda_{max\ emission}$=480 nm) and SYTO13 ($\lambda_{max\ emission}$=520 nm) were used for labeling cell nuclei (final concentration 2.0 μmol/l; Invitrogen, Breda, the Netherlands). Phycoerythrin (PE, $\lambda_{max\ emission}$=570 nm) conjugated rat antimouse CD11b (MAC-1α or CD18) was applied as marker for inflammatory cells such as mature macrophages,[19] monocytes, and granulocytes (final concentration 8 μg/ml; BD Biosciences, Alphen aan den Rijn, the Netherlands). Oregon Green 488 conjugated CNA35 (CNA35/OG488, $\lambda_{max\ emission}$=510 nm) was used for staining of collagen[13,18] (final concentration 1.5 μmol/l).

Two mounted and visualized arteries (ApoE$^{-/-}$ mice, 21 weeks) were also studied for lipid content. They were incubated overnight at 7 °C with the lipid marker oil red O (ORO, $\lambda_{max\ emission}$=560 nm; Fluka Chemie, Buchs, Switzerland) dissolved in 3.7% formaldehyde solution (Merck, Darmstadt, Germany) to a final concentration of 12 μmol/l.[14,20] ORO staining resulted in a significant reduction in fluorescence of previously applied labels and loss of cell viability. Furthermore, arterial rings (approximately 1 mm long) from 3 isolated and previously mounted arteries (ApoE$^{-/-}$ mice, 21 weeks) were labeled with ORO and transversally imaged for visualization of lipid content of plaques. After overnight incubation, arterial rings were labeled with SYTO13 (2.0 μmol/l, 30 minutes) and rings were cast in agarose gel (1.5% dissolved in HBSS, Gibco BRL 15510-027; Invitrogen, Breda, the Netherlands) as previously described.[14]

2.3 *Imaging*

The TPLSM[12,14] consisted of a Biorad 2100MP TPLSM (Biorad, Hemel Hempstead, UK) with a pulsed (100 fs at the entrance of the scan head) and mode-locked (800 nm) Ti:sapphire laser as the excitation source (Spectra Physics Tsunami, Mountain View, CA) connected to a Nikon E600FN microscope (60X, NA=1.0 water dipping objective; Nikon Corporation, Tokyo, Japan). Damage to the sample was avoided by keeping excitation laser power as low as possible.[21] On average, laser power of the excitation light was set at 15 mW for imaging in the tunica adventitia, 22 mW for imaging in the tunica media, and 30 mW for imaging in the tunica intima. In atherosclerotic lesions, laser power was maximized to 60 mW for imaging of plaque cores. Imaging rate was either 0.1 Hz with a pixel dwell time of 39 μs, or 0.3 Hz with a pixel dwell time of 0.12 μs combined with Kalman filtering for noise reduction (n=3 cycles). Fluorescent signals were detected by three photomultiplier tubes (PMTs): SYTO41, 460–480 nm (PMT I); CNA35/OG488, 520–550 nm (PMT II); CD11b/PE, 570–610 nm (PMT III); ORO, 540–610 nm (PMT III). From each PMT, separate images of 512*512 pixels were obtained, saved, and combined into a single RGB image. The filter setting for each PMT was tuned for minimal bleedthrough of fluorescent signal of the markers. Furthermore, the PMT gain was set to 100% in order to limit the required laser powers, while obtaining maximal signal intensity in deeper layers and atherosclerotic lesions of the arterial vessel wall.

Stacks of optical sections were collected for 3D reconstructions to screen for plaques in the entire mounted vessel; staining patterns in plaques differed from those of healthy carotid arteries. Plaque detection was checked using bright-field microscopy, where plaques showed up as dark and less translucent regions on a bright background. Image analysis was performed using Image-Pro Plus 6.0 and 3D-reconstructor 5.1 software package (Media Cybernetics Inc., Silver Spring, MDA).

2.3.1 *Relationship between CNA35/OG488 and CD11b/PE-positive cells*

To explore the relationship between collagen and inflammatory cells in initial, mild, and advanced plaques,[22] we assessed (1) the number of inflammatory (CD11b/PE-positive) cells per (100 μm)^3 plaque volume and (2) the contact ratio, being the relative number of inflammatory cells in contact with collagen. Plaque volumes were estimated using optical section thickness and surface area, excluding areas without fluorescent signal. The relationship between collagen (CNA35/OG488 labeled structures) and inflammatory (CD11b/PE-positive) cells in fibrous caps of mild and advanced lesions of ApoE$^{-/-}$ mice of both ages (n=14, only plaques with clearly visible fibrous cap) was scored: (0) <33% (1) 33–67% (2) >67% of inflammatory cells in contact with CNA35/OG488 labeled collagen.

2.3.2 *Cells in tunica adventitia*

Inflammatory (CD11b/PE-positive) cells and CD11b/PE-negative cells were counted in the tunica adventitia of athero-

Table 1 Mouse characteristics and presence of atherosclerotic lesions in C57BL6/J and ApoE$^{-/-}$ mice of 15 and 21 weeks.

	C57 (15 wks)	C57 (21 wks)	ApoE$^{-/-}$ (15 wks)	ApoE$^{-/-}$ (21 wks)
# mice (#carotids)	7(13)	7(12)	7(13)	6(11)
weight (g) (avg±SD)	26.5±1.9	29.2±2	27.8±2.6	30.2±2.4
# mice with plaque (#carotids with plaques)	0(0)	0(0)	5(9)	6(11)
Total # plaques in analyzed segments	—	—	12	21
Class 1 plaques (%)	—	—	7(58)	4(19)
Class 2 plaques (%)	—	—	5(42)	5(24)
Class 3 plaques (%)	—	—	0(0)	12(57)

sclerotic ($n=9$) and control ($n=12$) areas in the arterial wall. The ratio of inflammatory cells was assessed per total number of cells per (100 μm)^3 volume.

2.4 *Histology*

Histological sections were prepared to validate the penetration depth of TPLSM in plaques in mounted arteries. Subsequent to imaging of mounted arteries *ex vivo*, arteries (two C57BL6/J mice; two ApoE$^{-/-}$, all 21 weeks) were perfusion-fixated and processed to 5 μm-thick histological sections and stained for collagen with Picrosirius Red[23] (0.1%, Klinipath, Duiven, the Netherlands). Histological sections were imaged using a Leica DM 5000B microscope (60X oil objective; NA=1.4) and a Leica DC300FX digital camera (Leica Microsystems GmbH, Wetzlar, Germany).

2.5 *Statistics*

Data are presented as medians (M) with interquartile ranges (IQR): M [IQR]. Results were tested for significance using the Mann–Whitney test. A value of $p<0.05$ was considered statistically significant. SPSS 13.0 software package (SPSS Inc., Chicago, IL) was used for statistical analysis.

3 Results

3.1 *Carotid Arteries of C57BL6/J Mice*

Carotid arteries of C57BL6/J mice contained no lesions (Table 1); The vessel wall structure was normal.[12] The tunica adventitia consisted of cells (SYTO41) embedded in collagen (CNA35/OG488). The vSMCs in the tunica media were homogeneously distributed and arranged perpendicularly to the flow direction. Endothelial cell nuclei were homogeneously distributed covering the tunica intima [Fig. 1(a)]. No inflammatory (CD11b/PE-positive) cells were present in or adhering to the arterial wall in any of the control arteries. Labeled collagen was only sparsely observed as local spots in the tunica intima (14% of the mice at 15 weeks 71% of the mice at 21 weeks), and not at all in the tunica media (see also Ref. 13). Hence, the endothelial cells appear nonactivated and nonpermeable for small molecules. The barrier function of internal elastic layer (IEL) and external elastic layer (EEL) appear intact, as deduced from the nonpermeability for the collagen probe.[13]

3.2 *Common Carotid Arteries of* ApoE$^{-/-}$ *Mice*

In the common carotid artery of both 15- and 21-week-old ApoE$^{-/-}$ mice, no atherosclerotic lesions were found; the tunica adventitia and media were undisturbed. However, a very thin sheet of collagen [Fig. 1(b)] was observed between the endothelium and IEL of the tunica intima at both ages in 70% of the mice at 15 weeks and 100% of the mice at 21 weeks. In addition, inflammatory cells adhering to the luminal side of the endothelium were found in 85% of the mice at 15 weeks and 100% of the mice at 21 weeks [Fig. 1(c)]. The number of cells adhering to the endothelium increased with age from 0.2 [0–0.6] cells per (100 μm)^2 at 15 weeks to 0.6 [0.3–1.2] at 21 weeks ($p<0.05$). No inflammatory cells were present inside the arterial wall. These data suggest that endothelial cells were activated and permeable for the collagen probe, while IEL and EEL were still intact.

3.3 *Morphology of Lesion Development in the Carotid Bifurcation of* ApoE$^{-/-}$ *Mice*

In the carotid bifurcation of most ApoE$^{-/-}$ mice of both 15 and 21 weeks, atherosclerotic lesions were detected exhibiting strong collagen and cellular staining (72% and 100%, respectively; see Table 1). In all phases of lesion development, a thin sheet of collagen was clearly present in the tunica intima adjacent to the plaque area between endothelial cells and IEL. This indicates increased CNA35/OG488 permeability of endothelial cells in these regions, and possibly reflects increased collagen content in this layer. In young mice, plaques were of initial (class 1) or mild (class 2) type (Table 1). No advanced (class 3) plaques were found. In contrast, in mice of 21weeks, the majority of plaques were class 3 (Table 1).

In the initial phase of plaque development [class 1; see Fig. 1(d)], inflammatory cells were accumulated in the tunica intima underneath the endothelial cells. Furthermore, collagen in the lesions formed a thin sheet or local spots. In the tunica media underneath these initial plaques, the orientation and distribution of vSMCs were unaltered. No collagen or inflammatory cells were observed in the tunica media.

During further lesion progression, mild plaques developed (class 2). The first signs of a fibrous collagen-rich cap structure could already be observed at 15 weeks [Fig. 2(a); $n=5$ plaques; class 2]. In addition, infiltrated inflammatory cells were present in the tunica intima. In class 2 plaques at 21 weeks [Fig. 2(b)], the area of arterial wall affected by the atherosclerotic process appeared to be larger. Collagen-surrounded areas contained a combination of inflammatory cells (e.g., foam cells; $n=4$ plaques) or poorly fluorescent areas without visible structures (i.e., lesion cores; $n=2$ plaques) [Fig. 2(b)]. The tunica media underneath all class 2 plaques was free of inflammatory cells. Furthermore, vSMCs were homogeneously distributed and their orientation seemed unaffected. Collagen between vSMCs was not labeled.

Progression of a substantial number of lesions toward an advanced phase of atherosclerosis was only observed in

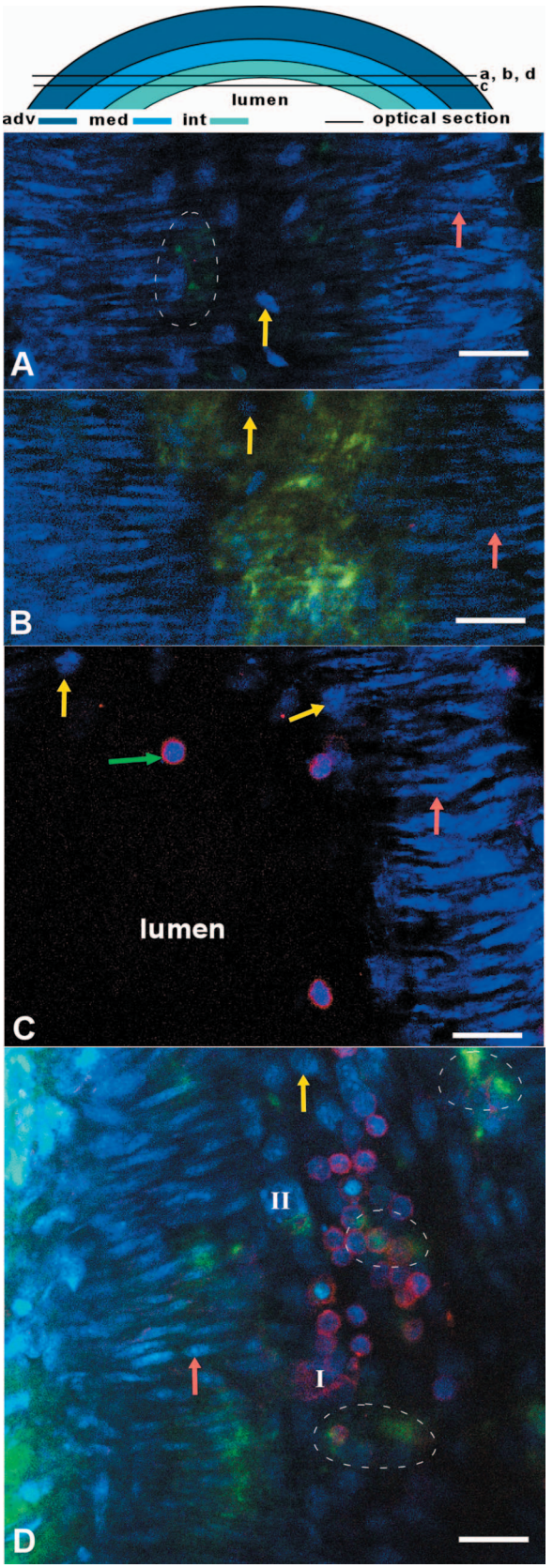

Fig. 1 Optical sections of tunica intima in a healthy common carotid segment of (a) C57BL6/J and (b)–(d) ApoE$^{-/-}$ mouse (each 21 weeks). Imaging depth of optical sections (a)–(d) in the vessel wall is around 70 μm (z=0 μm at outside of vessel wall). Arteries were stained for cell nuclei (SYTO41; blue), CNA35/OG488 (collagen, green), and anti-CD11b/PE (inflammatory cells, red). Section (c) was stained with SYTO41 and anti-CD11b/PE. Bars: 20 μm. Drawing at top indicates position of displayed sections. (a) Cell nuclei of vSMCs (pink arrow) and endothelial cells (yellow arrow) are clearly visible. Collagen (green) is only sporadically labeled (encircled by white dotted line) and inflammatory cells (red) are absent. At comparable sites in common carotid segments of ApoE$^{-/-}$ mice (b), the tunica intima contains a stronger collagen signal (green) between endothelial cells (yellow arrow) and vSMCs (pink arrow). (c) Inflammatory cells (green arrow) were detected adhering to endothelial cells (yellow arrow). (d) Typical example of a class 1 plaque present in carotid bifurcation of ApoE$^{-/-}$ mice of both ages. Several inflammatory cells (red) are clearly distinguishable in the distorted tunica intima underneath the endothelial cells (yellow arrow). Furthermore, a CD11b/PE-positive foam cell (I) and a CD11b/PE-negative foam cell (II) are visible. Local collagen spots (surrounded by white dotted lines) are noticeable in the lesion area. No collagen or inflammatory cells are visible between vSMCs (pink arrow) in tunica media. Distribution and orientation of vSMCs in the tunica media are unaltered.

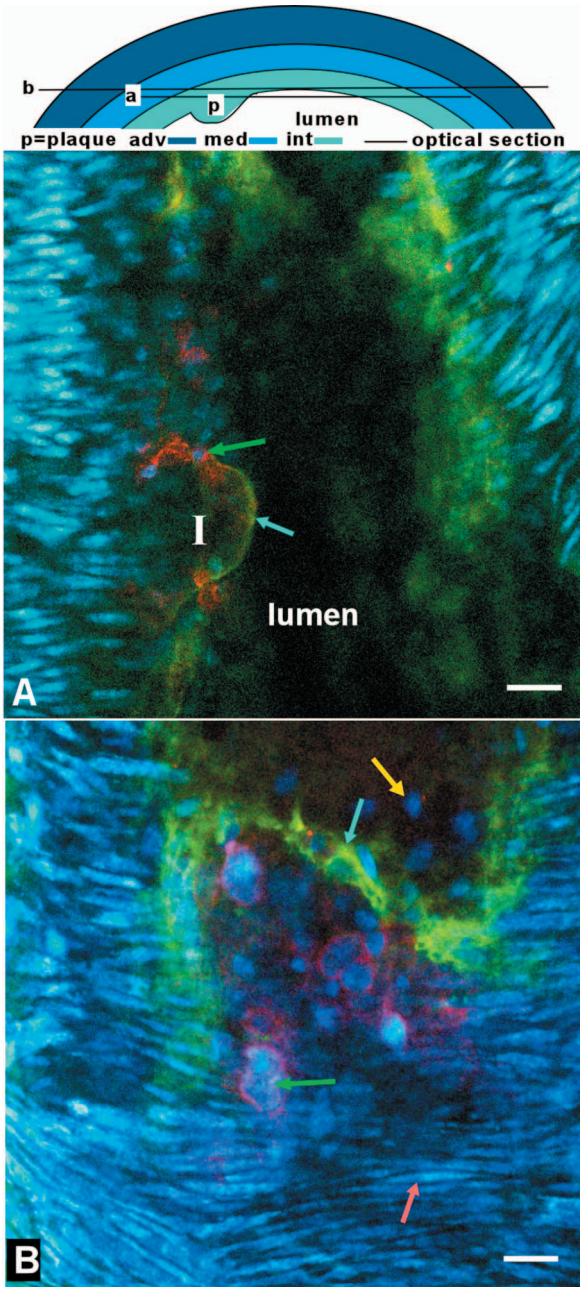

Fig. 2 Optical sections of typical mild plaques (class 2) as observed in tunica intima of ApoE$^{-/-}$ mice of (a) 15 and (b) 21 weeks. Both optical sections are acquired at $z \approx 70$ μm in the vessel wall ($z=0$ μm at outside of vessel wall). Arteries were labeled for nuclei (SYTO41; blue), collagen (CNA35/OG488; green), and inflammatory cells (anti-CD11b/PE; red). Drawing at top indicates position of both sections; bars: 20 μm. (a) Class 2 plaque in the carotid bifurcation of a young ApoE$^{-/-}$ mouse containing several inflammatory cells and large amounts of collagen. Collagen has fibrous caplike structure (blue arrow) with a small and weakly fluorescent area (I) inside that contains no collagen and only a few inflammatory cells, both typical properties of a small (necrotic) core. In surrounding arterial wall, strongly labeled collagen without a bulblike structure is observable. (b) Part of a typical class 2 plaque in carotid bifurcation of ApoE$^{-/-}$ mice (21 weeks), containing CD11b/PE-positive foam cells (green arrow) and round cells. Collagen is abundant, forming a fibrous cap (blue arrow) at edge of plaque. Adjacent to plaque area, endothelial cells are observable (yellow arrow). In the tunica media, vSMCs (pink arrow) are homogeneously distributed; their orientation is unaffected. No inflammatory cells or collagen are present in the tunica media.

21-week-old ApoE$^{-/-}$ mice (class 3; Table 1). In total, 60% of the advanced plaques [Figs. 3(a)–3(d)] consisted of strongly labeled collagen with a network-like appearance. Inside the collagen network, large lesion cores that contained only a little fluorescent signal were present. Infiltrated inflammatory cells were predominantly positioned at the edges between lesion cores and collagen network [Fig. 3(a)]. The shoulders of these class 3 plaques contained strongly labeled collagen [Fig. 3(b)]. In some shoulder areas of these plaques ($n=3$), strongly labeled collagen protruded beyond the edges of the lesion toward the healthy arterial wall [Fig. 3(b)].

Other class 3 plaques (40%) manifested as interconnected groups of smaller lesions with less evident plaque borders [Fig. 3(c)]. Such lesions consisted of many small lesion cores with weak fluorescent signal surrounded by large amounts of labeled collagen with a less defined network-like appearance. Many inflammatory cells of various sizes and shapes were observed throughout the lesion.

Application of a lipid stain (ORO) in mounted arteries with class 3 lesions revealed that the dark lesion cores inside plaques had a lipid-rich content [Fig. 4]. Imaging of the content of the cores in fresh (but not viable) arterial rings labeled with ORO [Figs. 4(b) and 4(c)] demonstrated that part of the lipids was situated inside (foam) cells as small droplets.

In the larger class 3 lesions ($n=4$), the fluorescent signal intensity drastically and abruptly decreased toward the lumen [Fig. 5(a)]. As a result, we were unable to visualize the complete lesion area in depth [Fig. 5(b)]; no fibrous cap or endothelial cell lining was visible using TPLSM. However, histological longitudinal sections stained for collagen revealed that such lesions do contain fibrous caps with endothelial cells [Fig. 5(c)].

The tunica media was affected in all class 3 plaques. Although no inflammatory cells were detected in this layer, the vSMC layer was disrupted and the orientation of vSMCs was altered [Fig. 3(d)]. Sometimes, collagen between vSMCs in these plaques was labeled, indicative of local disruption of IEL ($n=4$ plaques). The tunica adventitia of carotid arteries in both non-plaque regions [in ApoE$^{-/-}$ and wild-type mice; Fig. 6(a)] and plaque regions [in ApoE$^{-/-}$ mice; Fig. 6(b)] contained large amounts of collagen with a typical wavelike appearance. No apparent changes to the collagen structure were found between plaque regions and non-plaque regions. Furthermore, the tunica adventitia contained numerous inflammatory cells and non-inflammatory cells in both plaque and non-plaque regions.

3.4 *Inflammatory Cell Density*

During lesion development, the inflammatory cell density in plaques increased significantly with age ($p<0.05$) and with plaque progression ($p<0.01$; Table 2). The tunica media in plaque regions did not contain any inflammatory cells.

In the tunica adventitia, the total cell density tended to be higher in plaque regions than in non-plaque regions in mice of both ages {23.6 [31.1–17.8] cells per (100 μm^3) vs. 17.6 [23.6–13.3]; ($p=0.07$)}. The relative number of inflammatory cells in the tunica adventitia in mice of both ages was increased in plaque regions (0.58 [0.63–0.51]) compared to non-plaque regions (0.24 [0.36–0.18] $p<0.001$).

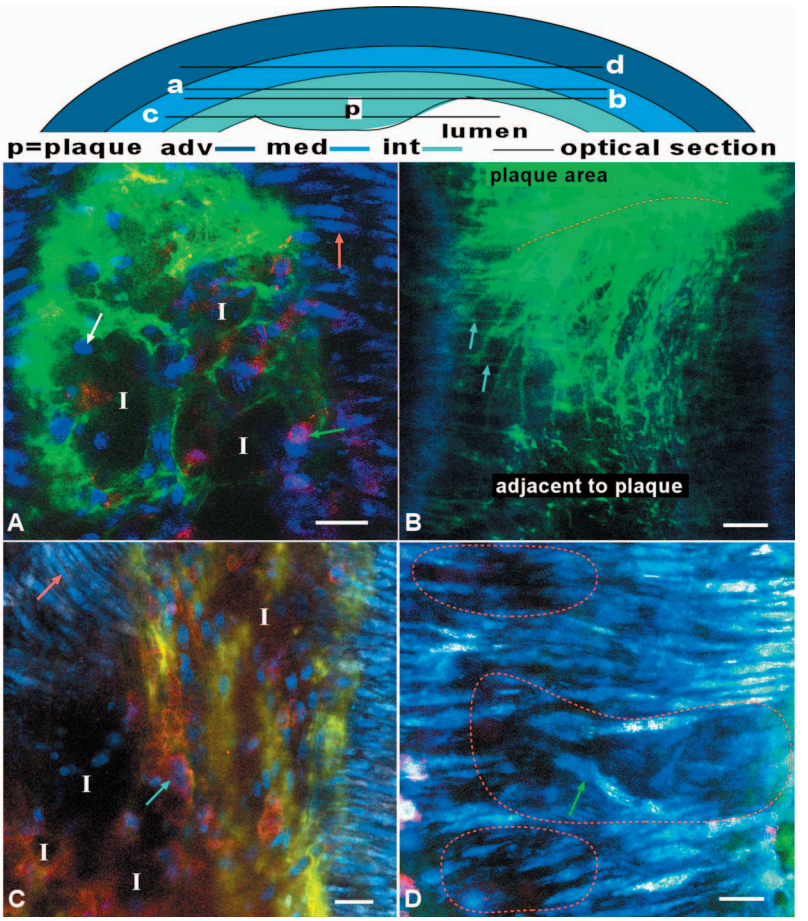

Fig. 3 Optical sections of advanced plaques (class 3) in (a)–(c) tunica intima and (d) tunica media of carotid bifurcations in ApoE$^{-/-}$ mice aged 21 weeks. Optical sections are acquired at (a)–(c) $z \approx 70$ μm or (d) $z \approx 55$ μm in the vessel wall ($z=0$ μm at outside of vessel wall). Arterial segments (a)–(d) were stained for nuclei (SYTO41; blue), collagen (CNA35/OG488; green), and inflammatory cells (anti-CD11b/PE; red). Segment (b) was stained for collagen only (CNA35/OG488). Bars: 20 μm; drawing at top indicates position of sections. (a) Advanced plaque with a network-like collagen structure, several lesion cores with weak fluorescent signal (I), and many inflammatory cells (green arrow) and non-inflammatory cells (white arrow). (b) Plaque shoulder (red dotted line) containing large amounts of collagen, which protrude into the area adjacent to the plaque (lower part of the section). Blue is autofluorescence of elastic laminae. Note that the fluorescence in (b) is optimized for the intensity of the adjacent area. Thus, the fluorescence in the shoulder is saturated. Class 3 plaques also appear as an interconnected group of smaller lesions with numerous inflammatory cells, and several lesion cores (c). Plaque borders and lesion cores (I) are less evident; collagen is abundant with less defined appearance. (d) The tunica media flanking advanced plaques contains areas with disrupted vSMCs layer (encircled by red dotted lines) and vSMC with altered orientation (green arrow).

3.5 *Relationship Between Collagen and Inflammatory Cells in Developing Plaques*

In plaques as a whole, the percentage of inflammatory cells in direct contact with collagen did not change significantly with age or plaque progression (Table 2). In fibrous caps, the median score of the association between collagen and inflammatory cells was significantly higher at 21 weeks (1.0 [2–1]) than at 15 weeks (0.5 [1–0]; $p < 0.05$). Note that fibrous caps were present only in class 2 and class 3 plaques. Moreover, class 3 plaques were only present in 21-week-old ApoE$^{-/-}$ mice.

4 Discussion

This study is the first to visualize and describe the association of collagen and inflammatory cells during plaque development in intact, still viable, mounted carotid arteries of ApoE$^{-/-}$ mice at the subcellular level. Visualization of mounted arteries with TPLSM enables further study of various aspects of atherosclerosis in a physiologically relevant environment.

The two-photon microscope setup used in this study did not allow complete visualization of the largest lesions (Fig. 6). The loss of signal deeper in these plaques meant that both the fibrous cap(s) and endothelial cell lining bordering the lumen could not be visualized. As a result, we were not able to quantify cell and collagen content in the largest lesion cores in mounted arteries. The question arises as to what causes this limited penetration depth. From experiments on healthy rabbit carotid and aortic arteries, which have similar structural properties, but a much thicker arterial wall (400 μm vs. 100 μm for healthy mouse carotids), we know that the penetration depth can be up to 250–300 μm. Therefore, we feel that the limited penetration depth of 100 μm in diseased arteries is not caused by fundamental scattering limitations.[24] Interest-

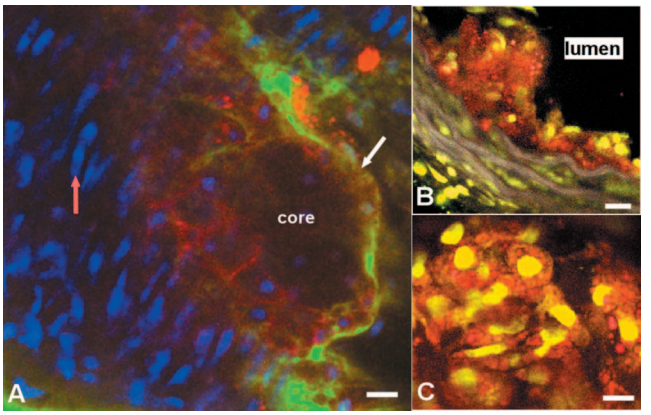

Fig. 4 (a) Mounted artery of 21-week-old ApoE$^{-/-}$ mice, containing a class 3 plaque in the bifurcation, labeled for nuclei (SYTO41; blue), collagen (CNA354/OG488; green), and lipids (ORO; red). Bars: 10 μm. Image is acquired at $z=74$ μm (outside vessel wall $z=0$ μm). Note the lipid content in core of the lesion, collagen in the fibrous cap (white arrow), and vSMCs in tunica media (red arrow). (b), (c) Optical sections of fresh arterial rings stained with ORO and SYTO13 (nuclei, green) further demonstrate that lipids (red) are mainly situated as small droplets inside cells in the lesion cores. As in mounted atherosclerotic arteries, the maximal depth of imaging in fresh arterial rings inside the plaque core was limited to $z_{max} \approx 100$ μm.

ingly, already in healthy arteries we deduced relevant spherical aberrations[25,26] from a change in intensity and resolution deeper in the arterial wall. When determining the PSF from subresolution beads (not shown), we found an increase by a factor of 1.3 to 1.5 of the PSF inside the healthy arterial lumen when compared with the PSF at the outside of the artery ($0.5\times0.5\times2.1$ μm and $0.4\times0.4\times1.4$ μm, respectively, in the x, y, and z directions). Local accumulation of high-refractive-index plaque components like lipids will likely induce even much stronger and local spherical aberrations. In combination with enhanced absorption, this will seriously hamper penetration depth[25,26] through these local structures.

While the cause of limited penetration depth in diseased arteries is thus rather fundamentally related to plaque composition, enhancing penetration depth of two-photon laser excitation light by narrowing pulse width in the focal plane (by precompensation at the entrance of the scan head), and thus increasing the probability of two-photon excitation, might enable imaging deeper in intact advanced plaques in the future,[27] provided that the cores are actually stained with the fluorochromes.

Intact, viable, and mounted carotid arteries of control C57BL6/J and atherosclerotic ApoE$^{-/-}$ mice were visualized three-dimensionally at a subcellular level. Control vessels had intact endothelium without adhering blood cells. In ApoE$^{-/-}$ mice, the endothelium was activated, even at non-atherosclerosis-prone sites, as indicated by the presence of adhering inflammatory cells and the increase of labeled collagen in the tunica intima. In plaques, located exclusively in the carotid bifurcation of ApoE$^{-/-}$ mice, inflammatory cell density increased with age and plaque progression. In fibrous caps, direct contact between inflammatory cells and collagen increased with age. However, in plaques as a whole, aging or plaque progression did not alter the direct relationship between inflammatory cells and collagen. The increased number of inflammatory cells in the tunica adventitia of lesions is remarkable since inflammatory cells were absent in the tunica media of these lesions. Since the vaso vasorum generally is absent in murine plaques at this stage,[28,29] this suggests that the increase might be caused by local inflammatory processes from surrounding tissues.

In contrast to control mice, endothelial cells appeared to be activated in carotid arteries of ApoE$^{-/-}$ mice, both in and outside the lesion area, and also in the common carotid artery. It is unlikely that this activation resulted from the mounting procedure since it was not observed in control vessels that were treated similarly.

The observation that the number of adhering cells was higher at 21 than at 15 weeks implies that the level of endothelial activation depends on increased duration of western diet and/or age. Besides increased cell adhesion, increased collagen labeling was observed in the tunica intima of common carotid arteries in ApoE$^{-/-}$ mice at both ages. This is in line with previous findings on properties of the collagen label CNA35/OG488 in (atherosclerotic) arteries,[13] implying that this is most probably caused by increased permeability of the endothelium as a consequence of factors like hypercholesteremia.[30] However, it cannot be excluded that intimal collagen content itself increased as well. The combination of increased collagen labeling in the tunica intima and adhesion of inflammatory cells to the endothelium at sites where no lesions are formed or present suggests that all

Table 2 Intraplaque inflammatory cell density and association between inflammatory cells and collagen (medians with interquartile ranges).

	ApoE$^{-/-}$ 15 wks	ApoE$^{-/-}$ 21 wks	Plaques class 1	Plaques class 2	Plaques class 3
# Inflammatory cells/(100 μm)^3	15 [11–18.7]	20 [14.5–35][a]	12 [3–17]	18 [11–24.3][b]	27.5 [19.5–41.3][c,d]
Ratio	0.64 [0.55–0.67]	0.56 [0.46–0.64]	0.64 [0.63–0.67]	0.57 [0.51–0.65]	0.52 [0.39–0.64][d]

Ratio is number of inflammatory cells with collagen contact divided by total number of inflammatory cells.

[a] $p<0.05$ compared with 15-week-old ApoE$^{-/-}$;
[b] $p<0.05$ compared with class 1 plaques;
[c] $p<0.05$ compared with class 2 plaques.
[d] $p<0.05$ compared with class 1 plaques.

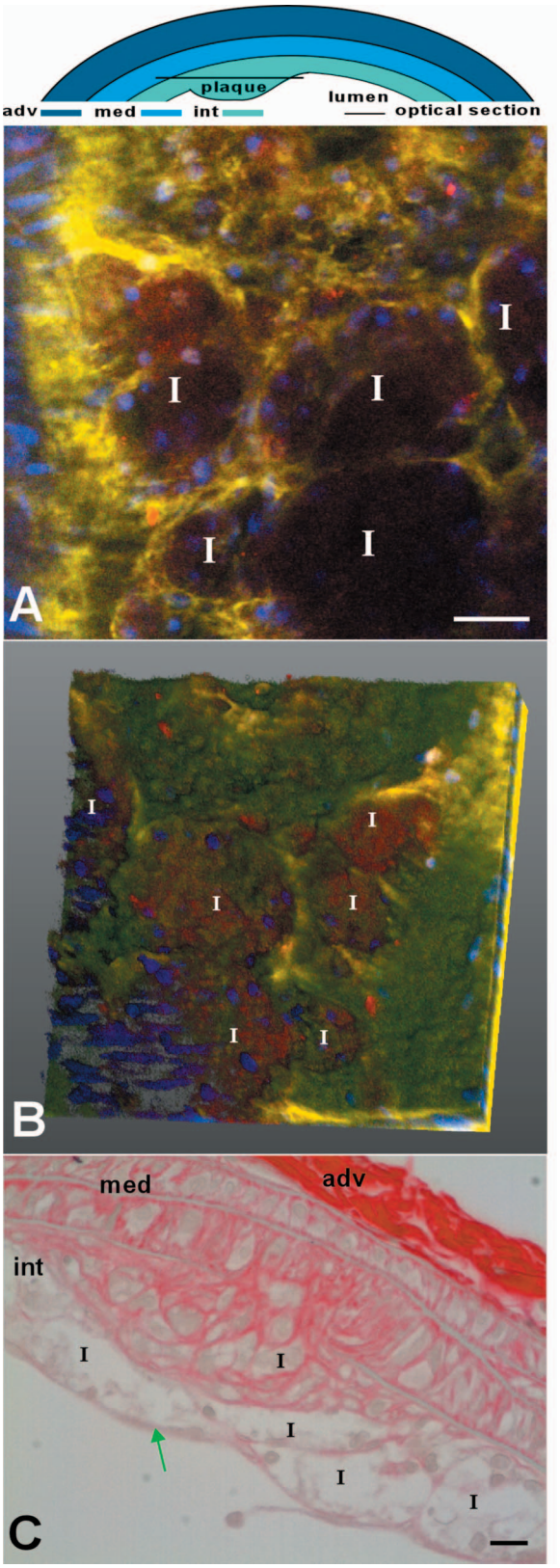

Fig. 5 (a) Optical section and (b) 3-dimensional reconstruction of a z-stack obtained in the tunica intima of class 3 plaque in a 21-weeks-old ApoE$^{-/-}$ mice. The z-stack in (b) runs over a region from $z=45$ to 84 μm with a step size of 1.5 μm in the arterial wall ($z=0$ μm at the outside of the vessel wall). Drawing at the top indicates position of section; bars: 20 μm. Artery was stained for collagen (CNA35/OG488; green), nuclei (SYTO41; blue), and lipids (ORO; red). (a) The lesion contains several lipid-rich lesion cores (I); the collagen has a network-like appearance. (b) The plaque lacks a fibrous cap. Unlike TPLSM images, histological sections of equivalent class 3 plaques (c) stained with picrosirius red (collagen, red) do contain a fibrous cap (green arrow) that consists of collagen. As in TPLSM images, lesion cores (I) are abundant.

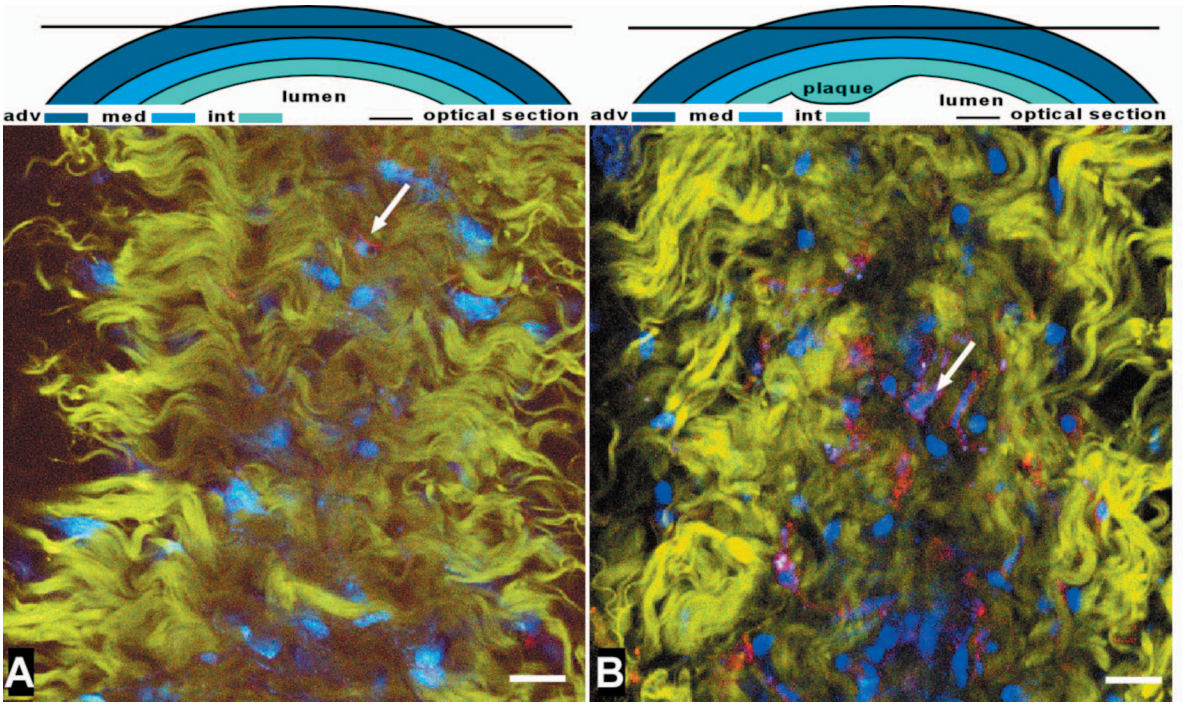

Fig. 6 Optical sections in (a) normal tunica adventitia of a C57BL6/J and (b) tunica adventitia of a plaque in an ApoE$^{-/-}$ mice, both 21 weeks old. Drawings on top indicate position of sections (depth ≈20 μm); bars: 20 μm. Arteries were stained for collagen (CNA35/OG488, green), nuclei (SYTO41, blue), and inflammatory cells (anti-CD11b/PE, red). In both sections, thin, undulating collagen fibers rearrange into thicker wavelike bundles of collagen. In between collagen, nuclei of cells are visible. (a) In the healthy artery, only a few inflammatory cells (white arrow) are present; (b) in the plaque, the number of inflammatory cells (white arrow) is much higher.

endothelial cells in carotid arteries of ApoE$^{-/-}$ mice on a western diet are activated.

Inflammatory cell density in plaques (carotid bifurcation) significantly increased with age and plaque progression. Simultaneously, a prominent network-like collagen structure inside the plaques and a collagen-rich fibrous cap developed, in line with literature stating that extracellular matrix components accumulate in the atherosclerotic vessel wall.[4,6] The contact ratio of inflammatory cell content and collagen in the entire plaque remained the same throughout plaque development. This is indicative of the development of the stable plaques.[1,6]

In the largest (class 3) plaques, collagen between vSMCs in the tunica media was labeled, indicating local disruption of IEL[13] as a consequence of plaque progression. In cores of such advanced lesions, co-localization of inflammatory cells and collagen could not be assessed in mounted arteries due to a lack of fluorescent signal. Observations in fresh arterial rings with additional labeling revealed that these cores contain large numbers of inflammatory cells (such as foam cells with many fat droplets) and only little collagen [Figs. 4(a)–4(c)].[31] This implies that especially in larger advanced plaques (which contain larger lesion cores) co-localization between inflammatory cells and collagen in the whole plaque may have been overestimated. In contrast to lesion cores, fibrous caps were found to be densely packed with collagen and little inflammatory cells, but co-localization of inflammatory cells and collagen did increase with age. This indicates that fibrous caps provide strength to the plaque while the cores become more and more unstable, suggesting that plaque destabilization is initiated from the core(s) of the plaque and progresses toward the outside borders such as the fibrous cap or the plaque shoulder. Yet, it is important to realize that presence of inflammatory cells alone does not provide any information regarding the activation state of such cells and, hence, the presence of active enzymes that can break down extracellular matrix components.

Acknowledgments

Gregorio Fazzi (Maastricht University, Department of Pharmacology) helped with histology, and Monica Breurken (Department of BME, Eindhoven University of Technology) helped with the preparation of CNA35/OG488. TPLSM was obtained via Grant no. 902-16-276 from the medical section of the Netherlands Organization for Scientific Research (NWO).

References

1. G. K. Hansson, "Inflammation, atherosclerosis, and coronary artery disease," *N. Engl. J. Med.* **352**(16), 1685–1695 (2005).
2. P. Libby, "Changing concepts of atherogenesis," *J. Intern Med.* **247**(3), 349–358 (2000).
3. E. Lutgens, R. J. van Suylen, B. C. Faber, M. J. Gijbels, P. M. Eurlings, A. P. Bijnens, K. B. Cleutjens, S. Heeneman, and M. J. Daemen, "Atherosclerotic plaque rupture: Local or systemic process?," *Arterioscler., Thromb., Vasc. Biol.* **23**(12), 2123–2130 (2003).
4. P. Libby, P. M. Ridker, and A. Maseri, "Inflammation and atherosclerosis," *Circulation* **105**(9), 1135–1143 (2002).
5. S. Katsuda and T. Kaji, "Atherosclerosis and extracellular matrix," *J. Atheroscler. Thromb.* **10**(5), 267–274 (2003).
6. S. Heeneman, J. P. Cleutjens, B. C. Faber, E. E. Creemers, R. J. van Suylen, E. Lutgens, K. B. Cleutjens, and M. J. Daemen, "The

dynamic extracellular matrix: Intervention strategies during heart failure and atherosclerosis," *J. Pathol.* **200**(4), 516–525 (2003).
7. A. J. Lusis, "Atherosclerosis," *Nature (London)* **407**(6801), 233–241 (2000).
8. A. D. Lucas and D. R. Greaves, "Atherosclerosis: Role of chemokines and macrophages," *Expert Rev. Mol. Med.* **3**, 1–18 (2001).
9. J. A. Rodriguez-Feo, J. P. Sluijter, D. P. de Kleijn, and G. Pasterkamp, "Modulation of collagen turnover in cardiovascular disease," *Curr. Pharm. Des.* **11**(19), 2501–2514 (2005).
10. Z. S. Galis and J. J. Khatri, "Matrix metalloproteinases in vascular remodeling and atherogenesis: The good, the bad, and the ugly," *Circ. Res.* **90**(3), 251–262 (2002).
11. W. Denk and K. Svoboda, "Photon upmanship: Why multiphoton imaging is more than a gimmick," *Neuron* **18**(3), 351–357 (1997).
12. R. T. Megens, S. Reitsma, P. H. Schiffers, R. H. Hilgers, J. G. De Mey, D. W. Slaaf, M. G. oude Egbrink, and M. A. van Zandvoort, "Two-photon microscopy of vital murine elastic and muscular arteries. Combined structural and functional imaging with subcellular resolution," *J. Vasc. Res.* **44**(2), 87–98 (2007).
13. R. T. A. Megens, M. G. A. oude Egbrink, J. P. M. Cleutjens, M. J. E. Kuijpers, P. H. M. Schiffers, M. Merkx, D. W. Slaaf, and M. A. M. J. van Zandvoort, "Imaging collagen in intact and viable healthy and atherosclerotic arteries using fluorescently-labeled CNA35: Towards molecular imaging of collagen in atherosclerotic plaques," *Mol. Imaging* **6**(4), 247–260 (2007).
14. M. van Zandvoort, W. Engels, K. Douma, L. Beckers, M. oude Egbrink, M. Daemen, and D. W. Slaaf, "Two-photon microscopy for imaging of the (atherosclerotic) vascular wall: A proof of concept study," *J. Vasc. Res.* **41**(1), 54–63 (2004).
15. D. E. Ferrara, D. Weiss, P. H. Carnell, R. P. Vito, D. Vega, X. Gao, S. Nie, and W. R. Taylor, "Quantitative 3D fluorescence technique for the analysis of *en face* preparations of arterial walls using quantum dot nanocrystals and two-photon excitation laser scanning microscopy," *Am. J. Physiol. Regulatory Integrative Comp. Physiol.* **290**(1), R114–123 (2006).
16. T. Boulesteix, A. M. Pena, N. Pages, G. Godeau, M. P. Sauviat, E. Beaurepaire, and M. C. Schanne-Klein, "Micrometer scale *ex vivo* multiphoton imaging of unstained arterial wall structure," *Cytometry, Part A* **69**(1), 20–26 (2006).
17. P. Maffia, B. H. Zinselmeyer, A. Ialenti, S. Kennedy, A. H. Baker, I. B. McInnes, J. M. Brewer, and P. Garside, "Images in cardiovascular medicine. Multiphoton microscopy for 3-dimensional imaging of lymphocyte recruitment into apolipoprotein-E-deficient mouse carotid artery," *Circulation* **115**(11), e326–328 (2007).
18. K. N. Krahn, C. V. Bouten, S. van Tuijl, M. A. van Zandvoort, and M. Merkx, "Fluorescently labeled collagen binding proteins allow specific visualization of collagen in tissues and live cell culture," *Anal. Biochem.* **350**(2), 177–185 (2006).
19. S. F. Bernatchez, M. R. Atkinson, and P. J. Parks, "Expression of intercellular adhesion molecule-1 on macrophages *in vitro* as a marker of activation," *Biomaterials* **18**(20), 1371–1378 (1997).
20. R. Koopman, G. Schaart, and M. K. Hesselink, "Optimisation of oil red O staining permits combination with immunofluorescence and automated quantification of lipids," *Histochem. Cell Biol.* **116**(1), 63–68 (2001).
21. K. Konig, "Multiphoton microscopy in life sciences," *J. Microsc.* **200**(Pt 2) 83–104 (2000).
22. M. J. Gijbels, M. van der Cammen, L. J. van der Laan, J. J. Emeis, L. M. Havekes, M. H. Hofker, and G. Kraal, "Progression and regression of atherosclerosis in APOE3-Leiden transgenic mice: An immunohistochemical study," *Atherosclerosis* **143**(1), 15–25 (1999).
23. M. Crisby, G. Nordin-Fredriksson, P. K. Shah, J. Yano, J. Zhu, and J. Nilsson, "Pravastatin treatment increases collagen content and decreases lipid content, inflammation, metalloproteinases, and cell death in human carotid plaques: Implications for plaque stabilization," *Circulation* **103**(7), 926–933 (2001).
24. P. Theer and W. Denk, "On the fundamental imaging-depth limit in two-photon microscopy," *J. Opt. Soc. Am. A* **23**(12), 3139–3149 (2006).
25. C. Y. Dong, K. Koenig, and P. So, "Characterizing point spread functions of two-photon fluorescence microscopy in turbid medium," *J. Biomed. Opt.* **8**(3), 450–459 (2003).
26. C. J. de Grauw, J. M. Vroom, H. T. M. van der Voort, and H. C. Gerritsen, "Imaging properties of two-photon excitation microscopy and effects of refractive-index mismatch in thick specimens," *Appl. Opt.* **38**(28), 5995–6003 (1999).
27. G. McConnel, "Improving the penetration depth in multiphoton excitation laser scanning microscopy," *J. Biomed. Opt.* **11**(5), 054020–054027 (2006).
28. M. R. Hayden and S. C. Tyagi, "Vasa vasorum in plaque angiogenesis, metabolic syndrome, type 2 diabetes mellitus, and atherosclerosis: A malignant transformation," *Cardiovasc. Diabetol.* **3**(1), 1 (2004).
29. A. C. Langheinrich, A. Michniewicz, D. G. Sedding, G. Walker, P. E. Beighley, W. S. Rau, R. M. Bohle, and E. L. Ritman, "Correlation of vasa vasorum neovascularization and plaque progression in aortas of apolipoprotein $E^{(-/-)}$ low-density lipoprotein$^{(-/-)}$ double knockout mice," *Arterioscler., Thromb., Vasc. Biol.* **26**(2), 347–352 (2006).
30. M. Simionescu, "Implications of early structural-functional changes in the endothelium for vascular disease," *Arterioscler., Thromb., Vasc. Biol.* **27**(2), 266–274 (2007).
31. H. C. Stary, A. B. Chandler, R. E. Dinsmore, V. Fuster, S. Glagov, W. Insull, Jr., M. E. Rosenfeld, C. J. Schwartz, W. D. Wagner, and R. W. Wissler, "A definition of advanced types of atherosclerotic lesions and a histological classification of atherosclerosis. A report from the Committee on Vascular Lesions of the Council on Arteriosclerosis, American Heart Association," *Circulation* **92**(5), 1355–1374 (1995).